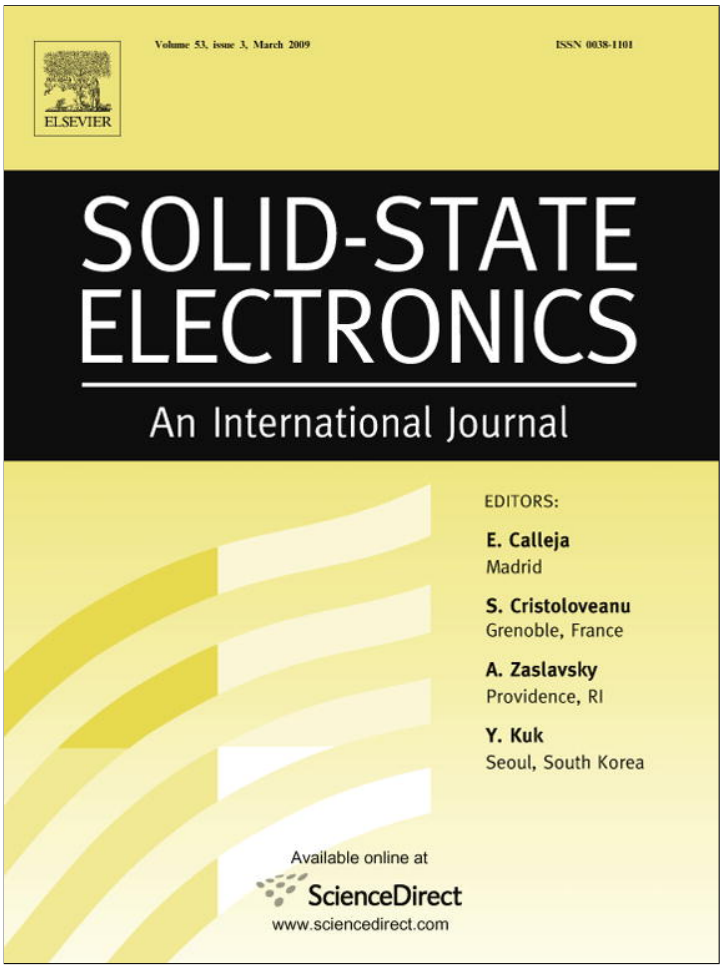

Solid-State Electronics 53 (2009) 251–255

Contents lists available at ScienceDirect

Solid-State Electronics

journal homepage: www.elsevier.com/locate/sse

The charge transport mechanism in silicon nitride: Multi-phonon trap ionization

A.V. Vishnyakov [a], Yu.N. Novikov [a,*], V.A. Gritsenko [a], K.A. Nasyrov [b]

[a] Institute of Semiconductor Physics, 13, Lavrentieva Ave., 630090 Novosibirsk, Russia
[b] Institute of Automation and Electrometry, 630090 Novosibirsk, Russia

ARTICLE INFO

Article history:
Received 20 February 2008
Received in revised form 17 June 2008
Accepted 16 July 2008
Available online 3 February 2009

The review of this paper was arranged by Prof. S. Cristoloveanu

Keywords:
Charge transport
Silicon nitride
Multi-phonon mechanism

ABSTRACT

The charge transport mechanism in amorphous silicon nitride, Si_3N_4, was experimentally examined to compare measured data with theoretical calculations made within the Frenkel model and the multi-phonon model of trap ionization. A good agreement between the experimental data and theoretical predictions could be achieved assuming the multi-phonon mechanism to be in effect. The widely accepted Frenkel model, although capable of explaining the measured data, fails to yield realistic values of the electron tunnel mass and attempt-to-escape factor.

1. Introduction

By definition, the conductivity of a perfect insulator at moderate temperatures should be extremely low. In 1916, Pool [1] was the first to show that the electrical conduction in mica increases in the presence of strong electric fields, with the increase following an exponential law. In 1938, Frenkel put forward a theoretical model to explain the exponential growth of conductivity with the field strength in dielectrics with traps [2]. Since then, the Frenkel model has been widely used to interpret charge transport-related phenomena in a wide class of dielectrics, including oxides, nitrides [3], high-*k* dielectrics [4], and ferroelectrics [5]. The multi-phonon model, an alternative to the Frenkel model, in which trap ionization was assumed to involve a multi-phonon process, was used to analyze the ionization of traps in semiconductors [6,7]. Not long ago it was argued, however, that trap ionization in semiconductors could be adequately understood in terms of the Frenkel model only in relatively low ($<10^3$ V/cm) electric fields [8].

Localization of electrons and holes is a common feature inherent to dielectrics and amorphous semiconductors [9]. For instance, amorphous silicon nitride, Si_3N_4, is known to localize electrons and holes, with the storage time being amazingly long (over 10 years at 400 K) [10]. Currently, the memory effect in Si_3N_4 is widely used in silicon-based nonvolatile flash memory devices [11,12]. The charge transport in metal–nitride–oxide–silicon (MNOS) structures with moderately thick Si_3N_4 layers (20–70 nm) is controlled by trapped charge in the Si_3N_4 bulk. The electric current across the dielectric as a function of applied voltage, and temperature is determined, therefore, by the corresponding dependences for the rate of trap ionization. Presently, it is generally accepted that the trap ionization mechanism in Si_3N_4 involves a Frenkel process, in which the electric field acts to lower the Coulomb barrier for trapped carriers, thus facilitating their migration through the dielectric [3]. The purpose of the present study was to investigate, both experimentally and theoretically, the mechanism of charge transport in Si_3N_4 over a wide range of temperatures and electric field intensities. To identify the mechanism underlying the charge transport in Si_3N_4, the data gained in the experiments were compared to predictions yielded by the Frenkel and the multi-phonon models of trap ionization.

2. Experimental

The metal–nitride–oxide–silicon (MNOS) structures used in the experiments presented were fabricated on n-type Czochralski-grown silicon wafers with a resistivity of 7.5 Ω cm. Ellipsometry was employed to measure the oxide and nitride thicknesses. A thin tunnel oxide layer, 1.8 nm thick, was thermally grown on the silicon wafers at 750 °C. A low pressure chemical vapor deposited (LPCVD) silicon nitride layer, 53 nm thick, was deposited onto the silicon at 760 °C. The SiH_2Cl_2/NH_3 ratio in the LPCVD process was 0.1. Aluminum electrodes with a square area of 5×10^{-3} cm^2 were prepared by means of photolithography.

* Corresponding author. Tel.: +7 383 3333 864; fax: +7 383 3332 771.
E-mail address: nov@isp.nsc.ru (Yu.N. Novikov).

0038-1101/$ - see front matter Crown Copyright © 2008 Published by Elsevier Ltd. All rights reserved.
doi:10.1016/j.sse.2008.07.005

3. Model

Fig. 1a shows the energy diagram of the MNOS structure. The energy parameters in the diagram, also used in the simulations described below, are as follows: silicon nitride gap $E_g = 4.5$ eV [10], barrier height for holes at the Si/SiO_2 interface $\varphi_h = 3.8$ eV [13], barrier height for holes at the Si/Si_3N_4 interface $\varphi_h = 1.5$ eV [14,15]. Fig. 1b and c illustrate the two-band model of electron and hole transport in Si_3N_4 under a positive bias voltage applied to the structure [16–18]. In this model, electron injection into the nitride from the negatively biased silicon substrate and hole injection from the positively biased Al contact are assumed. Free electrons can recombine with localized holes, and free holes can recombine with localized electrons in deep traps. The recombination cross-sections are assumed to be identical, $\sigma_r^e = \sigma_r^h = \sigma_r = 5 \times 10^{-13}$ cm^2 [17]. The charge transport in the nitride layer is assumed to be due to electron and hole drift in the dielectric under the applied electric field. In the model, the Shockley–Read–Hall approach for the trap occupation probability was adopted in combination with the Poisson equation and continuity equations for the hole and electron currents. Double carrier injection from the silicon substrate and from the Al contact was assumed to proceed by the modified Fowler–Nordheim mechanism. Thus, the following system of governing equations was adopted:

$$\frac{\partial n(x,t)}{\partial t} = \frac{1}{e}\frac{\partial j(x,t)}{\partial x} - \sigma_r \upsilon n(x,t)(N_t - n_t(x,t)) + n_t(x,t)P^{(n)}(x,t) - \sigma_r \upsilon n(x,t)p_t(x,t) \quad (1)$$

$$\frac{\partial n_t(x,t)}{\partial t} = \sigma \upsilon n(x,t)(N_t - n_t(x,t)) - n_t(x,t)P^{(n)}(x,t) - \sigma_r \upsilon p(x,t)n_t(x,t) \quad (2)$$

$$\frac{\partial p(x,t)}{\partial t} = \frac{1}{e}\frac{\partial j_p(x,t)}{\partial x} - \sigma \upsilon p(x,t)(N_t - p_t(x,t)) + p_t(x,t)P^{(p)}(x,t) - \sigma_r \upsilon p(x,t)n_t(x,t) \quad (3)$$

$$\frac{\partial p_t(x,t)}{\partial t} = \sigma \upsilon p(x,t)(N_t - p_t(x,t)) - p_t(x,t)P^{(p)}(x,t) - \sigma_r \upsilon p(x,t)n_t(x,t) \quad (4)$$

$$\frac{\partial F}{\partial x} = -e\frac{(n_t(x,t) - p_t(x,t))}{\varepsilon\varepsilon_0} \quad (5)$$

Here, n, N_t, and n_t are the densities of free electrons, electron traps, and occupied electron traps, respectively; p and p_t are the densities of free and trapped holes, respectively. The number of traps for electrons and holes was assumed to be identical, $N_t^e = N_t^h$. In (5) $F(x,t)$ is the local electric field, e is the electron charge, $\sigma = 5 \times 10^{-13}$ cm^2 is the cross-section for electron or hole capture at the traps, $\upsilon = 10^7$ cm/s is the electron and hole drift velocity, ε_0 is the dielectric constant, and $\varepsilon = 7.5$ is the Si_3N_4 low-frequency dielectric constant. The electron and hole drift currents are written as $j = en\upsilon$ and $j_p = -ep\upsilon$, and $P^{(n,p)}$ is the rate of trap ionization.

For the charge transport in silicon nitride, the crucial point is the mechanism of trap ionization. As mentioned previously, here we consider two models of trap ionization: (i) a modified Frenkel model with thermally assisted tunneling (TAT) and (ii) multi-phonon trap ionization. It should be noted that, presently, it is generally accepted that the charge transport in Si_3N_4 at high temperatures ($T > 300$ K) involves field-assisted tunneling of charge carriers between traps, or the Frenkel effect [2,3].

The rate of trap ionization, P, in the Frenkel model is given by

$$P_{FP} = \nu \exp\left(-\frac{W_t - \beta\sqrt{F}}{kT}\right); \quad \beta = \sqrt{\frac{e^3}{\pi\varepsilon_\infty\varepsilon_o}} \quad (6)$$

Here, W_t is the trap energy, β is the Frenkel constant, $\varepsilon_\infty = 4.0$ is the Si_3N_4 high-frequency dielectric permittivity, and ν is the attempt-to-escape factor.

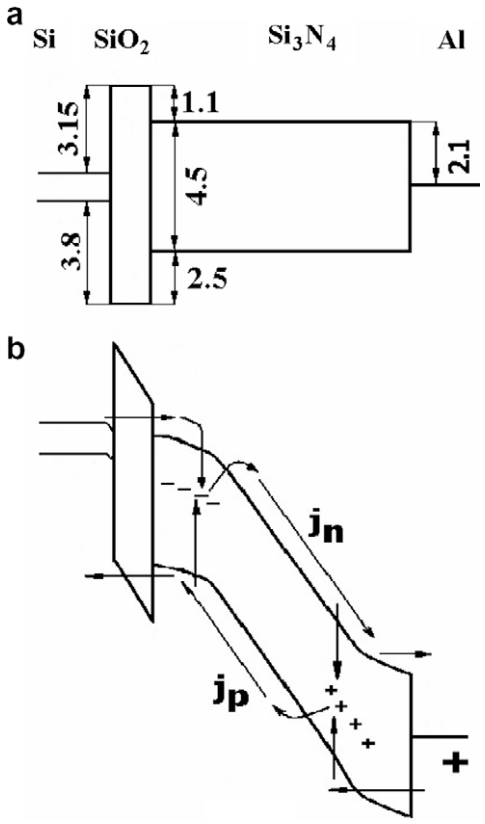

Fig. 1. Energy diagrams of the MNOS structure for the two-band model of charge transport in Si_3N_4: without applied voltage (a) and with a positive potential applied to the metal gate (b).

In addition to the classical Frenkel model, the thermally assisted tunnel mechanism for trap ionization was also considered. In the latter case, for a Coulomb center, the trap ionization probability is given by

$$P_{TAT} = \frac{\nu}{kT}\int_0^{W_t - \beta\sqrt{F}} dE \exp\left(-\frac{E}{kT} - \frac{2}{\hbar}\int_{x_1}^{x_2} dx\sqrt{2m^*(eV(x) - E)}\right)$$
$$V(x) = W_t - \frac{e}{4\pi\varepsilon_\infty\varepsilon_0 x} - Fx \quad (7)$$

Here E is the excited energy level (see Fig. 2), m^* is the tunnel effective mass, and x_1 and x_2 are the classical turning points,

$$x_{1,2} = \frac{1}{2}\frac{W_t - E}{eF}\left(1 \mp \left(1 - \frac{eF}{\pi\varepsilon_\infty\varepsilon_0(W_t - E)^2}\right)^{1/2}\right) \quad (8)$$

The electron tunneling is treated here within the semi-classical approximation, and the integral over x can be expressed in terms of elliptic integrals. Thus, the total rate of trap ionization in the modified Frenkel model is

$$P = P_{FP} + P_{TAT} \quad (9)$$

The model assuming the multi-phonon mechanism to be in effect will now be discussed. Following Makkram-Ebeid and Lannoo [6], phonon-coupled traps are considered here. Each such trap presents an "oscillator", or a "core", embedded in the nitride lattice, which can capture an electron (electron trap) or a hole (hole trap). The trap is completely defined by the phonon energy, $W_{ph} = \hbar\omega$, the thermal ionization energy, W_T, and the optical ionization energy, W_{opt}; the meaning of these parameters is clear from Fig. 2. The trap can undergo ionization, i.e., decomposition into an empty "core" and a free carrier, with the sum of their energies being equal to

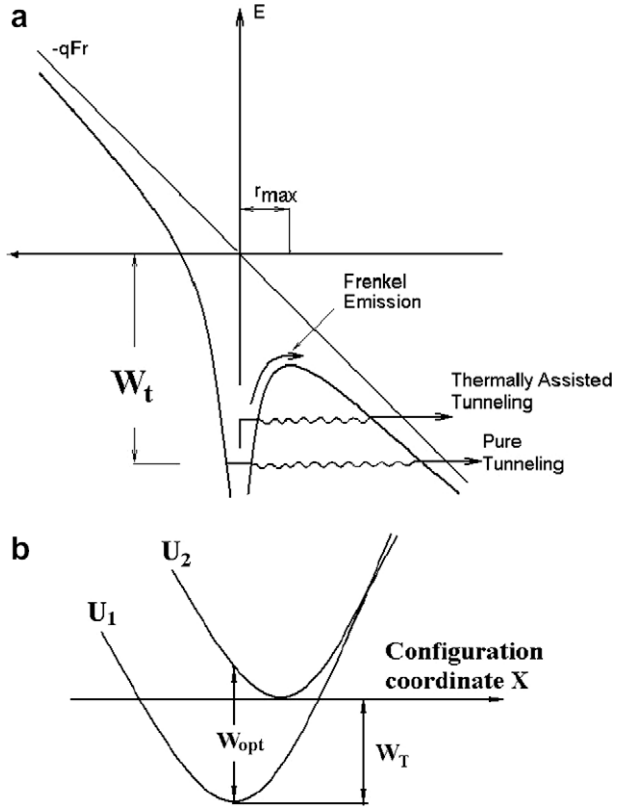

Fig. 2. Coulomb-trap ionization in a high electric field: pure tunneling at low temperatures and high fields; thermally assisted tunneling at middle temperatures; and thermal ionization (Frenkel emission) at low fields (a). The configuration diagram for the trap in the multi-phonon model (b).

the initial energy of the filled trap. Following the ionization process, the "core" enters an intermediate exited state, with the excess energy being spent to excite lattice vibration modes. For such traps, the quantum theory [6] yields the following equation for the rate of trap ionization

$$P = \sum_{n=-\infty}^{+\infty} \exp\left[\frac{nW_{ph}}{2kT} - S\coth\frac{W_{ph}}{2kT}\right] I_n\left(\frac{S}{\sinh(W_{ph}/2kT)}\right) P_i(W_T + nW_{ph})$$
$$P_i(W) = \frac{eF}{2\sqrt{2m^*W}} \exp\left(-\frac{4}{3}\frac{\sqrt{2m}}{\hbar eF}W^{3/2}\right), \quad S = \frac{W_{opt} - W_T}{W_{ph}} \tag{10}$$

Here, I_n is the modified Bessel function, and the value $P_i(W)$ is the rate of tunnel escape of the charge carrier through a triangular barrier of height W.

4. Comparison of experimental to theoretical data

Two sets of experiments were performed to gain information about the trap ionization mechanism. In experiments of the first type, the electric current across the silicon nitride layer was measured versus temperature at fixed positive bias voltages applied to the structure. In experiments of the second type, the electric current was measured as a function of applied bias voltage. The experimental current-vs-temperature curves taken at various fixed positive voltages applied to the Al contact are shown in Fig. 3 as plotted in the Arrhenius coordinates $\log J - T^{-1}$. The current is approximately constant at temperatures below 200 K, exhibiting a rapid growth at higher temperatures ($T > 200$ K).

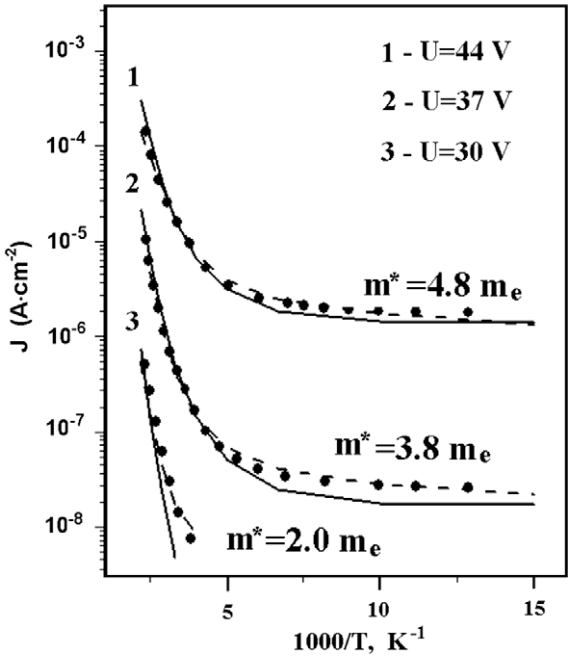

Fig. 3. The current–temperature characteristics of MNOS under different positive voltages (with respect to Al). Dots – experimental data, dashed curves – theoretical data predicted by the Frenkel model (with the effective masses indicated at each bias voltage), solid curves – theoretical data predicted by the multi-phonon model. MNOS geometry: tunnel oxide thickness d_{ox} = 1.8 nm, nitride thickness d_N = 53 nm.

First, an attempt was made to fit the experimental curves with data calculated by the modified Frenkel model (including TAT). Fitting the high-temperature portions of the experimental current-vs-temperature curves yields a trap energy of W_t = 1.2 eV and equal electron and hole trap densities of $N_t = 7 \times 10^{19}$ cm^3. However, the deduced attempt-to-escape factor turned out to be unreasonably low, $\nu = 6 \times 10^6$ s^{-1}, contrary to the original paper by Frenkel in which this factor was estimated as $\nu \approx W_t/h \approx 10^{15}$ s^{-1} [2]. Previously, for the Frenkel effect in Si_3N_4, attempt-to-escape factor values ranging in the interval $\nu = 10^6$–10^9 s^{-1} were reported [18,19]. Fitting the low-temperature portions of current-vs-temperature curves allows one to determine the effective mass of tunneling charge carriers. To obtain a satisfactory fit of our experimental curves taken at different bias voltages with the modified Frenkel model, we were forced to vary the tunnel mass in the interval from 2.0m_e to 4.8m_e ($m_e^* = m_h^* = 4.8\ m_e$ for V = 44 V, 3.8m_e for V = 37 V, and 2.0m_e for V = 30 V). These mass values are one order of magnitude larger than the experimentally determined electron and hole tunnel masses in Si_3N_4, 0.3–0.6m_e [14–16,20,21]. Thus, we can conclude that the modified Frenkel model, although capable of furnishing a formal description of the electron and hole transport in Si_3N_4, leads to an unreasonably low value of the attempt-to-escape factor, and to an abnormally large effective mass of tunneling charge carriers.

In fitting the experimental data with the model assuming phonon-assisted trap ionization, the varied parameters were W_{opt}, W_T, and W_{ph}. For the effective masses of tunneling charge carriers, a fixed value of $m_e^* = m_h^* = 0.5m_o$ was adopted. Here, a fairly good agreement between the theory and the experiment could be achieved, with the parameter values obtained being W_{opt} = 2.8 eV, W_T = 1.4 eV, and W_{ph} = 60 meV (see Fig. 3).

The current–voltage curves for positive bias voltages applied to the metal are shown in Fig. 4. Here, the best agreement between the experimental curves and the data calculated by the multi-phonon model was achieved with the same trap parameters as those obtained from the best fit of the current–temperature curves.

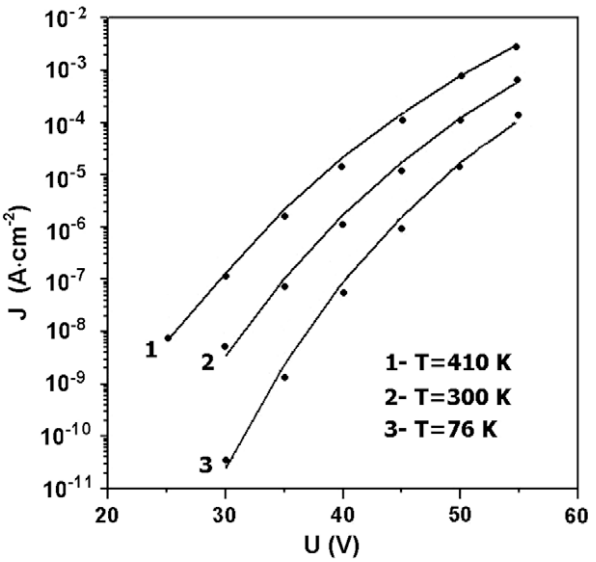

Fig. 4. Current–voltage characteristics of MNOS measured, at different temperatures, with positive potentials applied to the Al contact. Dots – experimental data, solid curves – theoretical data predicted by the multi-phonon model. MNOS geometry: tunnel oxide thickness d_{ox} = 1.8 nm, nitride thickness d_N = 53 nm.

5. Discussion

The best agreement between the experimental I–V–T data and theoretical calculations was obtained assuming identical parameters of electron and hole traps such as densities, cross-sections, optical energies, thermal energies, and effective tunnel masses. Previously, this assumption was adopted to explain the experimental data of [18], indicative of identical behaviors of hole- or electron-induced charges in discharge processes observed in nitride under different applied bias voltages. This hypothesis is also corroborated by the relatively weak dependence of the electric current on the bias-voltage polarity in MNOS structures [3,16].

The value of the attempt-to-escape factor determined from the best fit of our experimental data with the modified Frenkel model, $\nu = 6 \times 10^6\ s^{-1}$, seems to be unrealistically low. Previously, values of the attempt-to-escape factor for Si_3N_4 traps ranging in the interval $\nu = 10^6$–$10^9\ s^{-1}$ were reported in [18,19]; these values, however, were also obtained assuming that the Frenkel mechanism controlled the charge transport in Si_3N_4. Contrary to these reports, experiments on MNOS discharge in retention mode [22] yield a value of $\nu = 10^{13}\ s^{-1}$ for the attempt-to-escape factor. Experiments with metal–oxide–nitride–oxide–semiconductor (MONOS) structures [23] yielded a value of $\nu = 2 \times 10^{13}\ s^{-1}$ for electron traps. In [24], the attempt-to-escape factors for electron and hole traps in silicon nitride were found to be $\nu = 4 \times 10^{13}\ s^{-1}$ and $\nu = 10^{14}\ s^{-1}$, respectively. In thermally stimulated current experiments with silicon oxide layers [25,26], frequency factors in the range of $(1.0–1.8) \times 10^{14}\ s^{-1}$ for traps in SiO_2 were established.

In the quasiclassical approximation [7], as well as in the quantum approach [6], the attempt-to-escape factor for phonon-coupled trap ionization can be written as

$$\nu = \frac{eF}{2\sqrt{2m^* W_{opt}}} \tag{11}$$

With a typical electric field strength of $F = 5 \times 10^6$ V/cm, the obtained optical trap ionization energy W_{opt} = 3 eV yields a value of $\nu = 6 \times 10^{13}\ s^{-1}$ for the attempt-to-escape factor, this value is close to the experimentally estimated factors in [22–26].

Fit of experimental data with the multi-phonon of trap ionization model yields a value two times greater than the thermal trap ionization energy, $W_{opt} \approx 2W_T$, for the optical trap ionization energy. This means that the energy barrier for the electron and hole capture by traps is close to zero. This fact agrees with the weak temperature dependence of the cross-sections of electron and hole capture in Si_3N_4 experimentally observed in [27].

Quantum-mechanical calculations show that the Si–Si bond in silicon nitride, which represents the smallest silicon cluster, can capture electrons and holes [28–30].

The phonon energy W_{ph} = 60 meV obtained in our simulations closely coincides with the phonon energy in amorphous silicon determined by means of Raman spectroscopy [31,32]. The coincidence of the trap phonon energy with the amorphous silicon phonon energy suggests that amorphous silicon nanoclusters possibly act as electron and hole traps in silicon nitride. This hypothesis was previously advanced in [33]. The quantum confinement in amorphous silicon quantum dots embedded in silicon nitride was observed in optical absorption and photoluminescence experiments [34,35]. Recently, it was shown directly that amorphous Si nanoclusters indeed can capture electrons and holes in silicon nitride [36].

The data obtained in the present study allow no definite choice to be made in favor of the silicon cluster or Si–Si bond model. A detailed study of the nature of traps responsible for the memory effect in silicon nitride falls outside the scope of the present study.

6. Conclusions

The Frenkel model of Coulomb-trap ionization, in combination with the two-band conduction model, although capable of offering a formal description to the experimental J–V–T data for Si_3N_4, fails to yield realistic values for the effective electron tunnel mass and attempt-to-escape factor, which turn out to be, respectively, too large and too low in the offered description. On the other hand, the charge transport in silicon nitride can be adequately understood, with physically reasonable values of carrier masses and trap energies, assuming the two-band conduction model and the multi-phonon mechanism of trap ionization. A best fit of the experimental data can be achieved assuming constant parameter values for electron and hole traps such as densities, optical and thermal ionization energies, and phonon energies. The phonon energy deduced from our data coincides with the phonon energy in amorphous silicon, providing support to the assumption that it is amorphous silicon nanoclusters that act as the electron and hole traps in silicon nitride.

Acknowledgements

This work was supported by the Siberian Division of the Russian Academy of Sciences (Project No. 70), by the Russian Foundation for Basic Research (Grant No. 06-02-16621a), and by the National Program for Tera-Level Nanodevices of the Korea Ministry of Science and Technology as one of the 21st Century Frontier Programs.

References

[1] Pool HH. On the dielectric constant and electrical conductivity of mica in intense fields. Philos Mag 1916;34(187):112–28.
[2] Frenkel J. On pre-breakdown phenomena in insulators and electronic semiconductors. Phys Rev 1938;54:647–8.
[3] Sze SM. Physics of semiconductor devices. New York: Wiley; 1985.
[4] Zhu WJ, Ma TP, Tamagawa T, Kim J, Di Y. Current transport in metal/hafnium oxide/silicon structure. IEEE Electron Dev Lett 2002;23:97–100.
[5] Laha A, Krupanidhi SB. Leakage current conduction of pulsed excimer laser ablated $BaBi_2Nb_2O_9$ thin films. J Appl Phys 2002;92(1):415–20.
[6] Makram-Ebeid SS, Lannoo M. Quantum model for phonon-assisted tunnel ionization of deep levels in a semiconductor. Phys Rev B 1982;25:6406–24.
[7] Abakumov VN, Perel VI, Yassievich IN. Non-radiative recombination in semiconductors. In: Agranovich VM, Maradudin AA, editors. Modern

problems in condensed matter science. Amsterdam (The Netherlands); 1991. p. 9–99.
[8] Ganichev SD, Ziemann E, Prettl W, Yassievich IN, Istratov AA, Weber ER. Distinction between the Pool–Frenkel and tunneling models of electric-field-stimulated carrier emission from deep levels in semiconductors. Phys Rev B 2000;61:10361–5.
[9] Mott NF, Davis EA. Electron processes in non-crystalline materials. Oxford: Clarendon Press; 1979.
[10] Gritsenko VA. Electronic structure and optical properties of silicon nitride. In: Silicon nitride in electronics. New York: Elsevier; 1986.
[11] Gritsenko VA, Nasyrov KA, Novikov YN, Aseev AL, Yoon SY, Lee EH, et al. A new low-voltage fast SONOS memory with high-*k* dielectric. Solid-State Electron 2003;47:1651–6.
[12] Lee CH, Hur SH, Shin YC, Choi JH, Park DG, Kim K. Charge-trapping device structure of SiO_2/SiN/high-*k* dielectric Al_2O_3 for high-density flash memory. Appl Phys Lett 2005;86:152908–12.
[13] Goodman AM. Photoemission of holes from silicon into silicon dioxide. Phys Rev 1966;152:780–4.
[14] Gritsenko VA, Shaposhnikov AV, Kwok WM, Wong H, Zhidomirov GM. Valence band offset at silicon/silicon nitride and silicon nitride/silicon oxide interfaces. Thin Solid Films 2003;437:135–8.
[15] Gritsenko VA, Meerson EE, Morokov YN. Thermally assisted tunneling at Au–Si_3N_4 interface and energy band diagram of metal–nitride–oxide–semiconductor structures. Phys Rev 1998;57:R2081–3.
[16] Ginovker AS, Gritsenko VA, Sinitsa SP. Two band conduction of amorphous silicon nitride. Phys Status Solidi 1974;26:489–93.
[17] Gadiyak GV, Obrecht MA, Sinitsa SP. Calculation of bipolar injection and recombination in MNOS structure. Microelectronics 1985;14:512–6 [Soviet, in Russian].
[18] Gritsenko VA, Meerson EE, Travkov IV. Nonstationary electrons and holes transport by depolarization of MNOS structures: experiment and numerical simulation. Microelectronics 1987;16:42–9 [Soviet, in Russian].
[19] Bachhofer H, Reisinger H, Bertagnolli E, Philipsborn H. Transient conduction in multidielectric silicon–oxide–nitride–oxide semiconductor structures. J Appl Phys 2001;89(5):2791–800.
[20] Miyazaki S, Ihara Y, Hirose M. Resonant tunneling through amorphous silicon–silicon nitride double-barrier structures. Phys Rev Lett 1987;59:125–7.
[21] Yeo YC, Lu Q, Lee WC, King TJ, Hu C, Wang X, et al. Direct tunneling gate leakage current in transistors with ultrathin silicon nitride gate dielectric. IEEE Electron Dev Lett 2000;21:540–2.
[22] Lundkvist L, Lundstrom I, Hansson B. Discharge of MNOS structures at elevated temperatures. Solid-State Electron 1976;9:221–7.
[23] Roy A, White MH. Determination of the trapped charge distribution in scaled silicon nitride MONOS nonvolatile memory devices by tunneling spectroscopy. Solid-State Electron 1991;34:1083–9.
[24] Aozasa H, Fujiwara I, Nakamura A, Komatsu Y. Analysis of carrier traps in Si_3N_4 in oxide/nitride/oxide for metal/oxide/nitride/oxide/silicon nonvolatile memory. Jpn J Appl Phys 1999;38:1441–7.
[25] Miller SL, Fleetwood DM, McWhorter PJ. Determining the energy distribution of traps in insulating thin films using the thermally stimulated current technique. Phys Rev Lett 1992;69:820–3.
[26] Fleetwood DM, Winokur PS, Shaneyfelt MS, Riewe LC, Flament O, Pailet P, et al. Effect of isochronal annealing and irradiation temperature on radiation-induced trapped charge. IEEE Trans Nucl Sci 1998;45:2366–74.
[27] Hampton FL, Cricci JR. Steady-state electron and hole space charge distribution in LPCVD silicon nitride films. Appl Phys Lett 1979;35:802–4.
[28] Gritsenko VA, Morokov YN, Novikov YN, Wong H. Simulation of Si–Si bond electronic structure in Si_3N_4 and SiO_2. Microelectron Reliab 1998;38:1457–64.
[29] Gritsenko VA, Novikov YN, Shaposhnikov AV, Wong H, Zhidomirov GM. Capturing properties of three-fold coordinated silicon atom in silicon nitride: a positive correlation energy model. Phys Solid State 2003;45:1934–7.
[30] Petersen M, Roizin Y. Density functional theory study of deep traps in silicon nitride memories. Appl Phys Lett 2006;89:053511–3.
[31] Smith JEJ, Brodsky MH, Crowder BL, Nathan MI, Pinczuk A. Raman spectra of amorphous Si and related tetrahedrally bonded semiconductors. Phys Rev Lett 1971;26:642–6.
[32] Giorgis F. Optical absorption and photoluminescence properties of a-$Si_{1-x}N_x$:H films deposited by plasma-enhanced CVD. Phys Rev B 2000;61:4693–8.
[33] Gritsenko VA, Gritsenko DV, Novikov YN, Kwok PBM, Bello I. Short range order, large scale potential fluctuations, and photoluminescence in amorphous SiN_x. J Exp Theor Phys 2004;98:760–8 (Soviet, in Russian).
[34] Park NM, Choi CJ, Seong TY, Park SJ. Quantum confinement in amorphous silicon quantum dots embedded in silicon nitride. Phys Rev Lett 2001;86:1355–7.
[35] Park NM, Kim TS, Park SJ. Band gap engineering of amorphous silicon quantum dots for light-emitting diodes. Appl Phys Lett 2001;78:2575–7.
[36] Park NM, Choi SH, Park SJ. Electron charging and discharging in amorphous silicon quantum dots embedded in silicon nitride. Appl Phys Lett 2002;81:1092–4.